Preclinical Development

Molecular Cancer Therapeutics

Thermal Targeting of an Acid-Sensitive Doxorubicin Conjugate of Elastin-like Polypeptide Enhances the Therapeutic Efficacy Compared with the Parent Compound *In Vivo*

Shama Moktan[1], Eddie Perkins[2], Felix Kratz[3], and Drazen Raucher[1]

Abstract

Elastin-like polypeptides (ELP) aggregate in response to mild hyperthermia, but remain soluble under normal physiologic conditions. ELP macromolecules can accumulate in solid tumors because of the enhanced permeability and retention effect. Tumor retention of ELPs can be further enhanced through hyperthermia-induced aggregation of ELPs by local heating of the tumor. We evaluated the therapeutic potential of ELPs in delivering doxorubicin in the E0771 syngeneic mouse breast cancer model. The ELP-Dox conjugate consisted of a cell-penetrating peptide at the N-terminus and the 6-maleimidocaproyl hydrazone derivative of doxorubicin at the C-terminus of ELP. The acid-sensitive hydrazone linker ensured release of doxorubicin in the lysosomes/endosomes after cellular uptake of the drug conjugate. ELP-Dox dosed at 5 mg doxorubicin equivalent/kg, extended the plasma half-life of doxorubicin to 5.5 hours. In addition, tumor uptake of ELP-Dox increased 2-fold when hyperthermia was applied, and was also enhanced compared to free doxorubicin. Although high levels of doxorubicin were found in the heart of animals treated with free doxorubicin, no detectable levels of doxorubicin were found in ELP-Dox–treated animals, indicating a correlation between tumor targeting and reduction of potential cardiac toxicity by ELP-Dox. At an optimal dose of 12 mg doxorubicin equivalent/kg, ELP-Dox in combination with hyperthermia induced a complete tumor growth inhibition, which was distinctly superior to free drug that only moderately inhibited tumor growth. In summary, our findings show that thermal targeting of ELP increases the potency of doxorubicin underlying the potential of exploiting ELPs to enhance the therapeutic efficacy of conventional anticancer drugs. *Mol Cancer Ther; 11(7); 1547–56. ©2012 AACR.*

Introduction

Chemotherapy is the mainstay for treating different types of breast cancer, especially in the neoadjuvant and palliative setting. The effective use of the most common chemotherapeutics, including doxorubicin, epirubicin, and paclitaxel, is however, often limited by their narrow therapeutic window, resulting in unacceptable toxicity, lack of tumor selectivity, and/or multidrug resistance. Targeting strategies that can deliver these drugs specifically to the tumor site are thus highly desirable and could result in an improved therapeutic index and concomitant benefit for the patient.

In this study, we describe a thermally responsive drug delivery platform technology based on the genetically engineered biopolymer elastin-like polypeptide (ELP) that targets solid tumors by combining passive tumor targeting strategy with the application of mild hyperthermia (1–6). ELPs undergo inverse phase transition at a specific temperature known as inverse transition temperature (T_t), below which they stay in solution and above which, due to collapse of the hydrophobic structure, form aggregates (7). This process is completely reversible. ELP is composed of repetitive units of Val-Prol-Gly-Xaa-Gly, in which Xaa is a guest residue that can be any amino acid except proline. The number of repeats as well as the molecular composition of Xaa directly influence the T_t of ELP (8). Compared with low-molecular weight drugs, ELPs remain in blood circulation with a half-life of approximately 8.7 hours (9), sufficient for passive tumor targeting through the enhanced permeability and retention effect characterized by hypervasculature and an impaired lymphatic drainage system of the tumor tissue (10), and thermally responsive ELPs can be actively targeted to the tumor tissue by application of local hyperthermia on the tumor (6). ELPs are conveniently expressed in *Escherichia coli* and purified in high yields using inverse thermal cycling (11), and they have a defined molecular

Authors' Affiliations: Departments of [1]Biochemistry and [2]Neurosurgery, University of Mississippi Medical Center, Jackson, Mississippi; and [3]Division of Macromolecular Prodrugs, Tumor Biology Center, Freiburg, Germany

Note: Supplementary data for this article are available at Molecular Cancer Therapeutics Online (http://mct.aacrjournals.org/).

Corresponding Author: Drazen Raucher, Department of Biochemistry, University of Mississippi Medical Center, 2500 North State Street, Jackson, MS 39216. Phone: 601-985-1510; Fax: 601-984-1501; E-mail: draucher@umc.edu

doi: 10.1158/1535-7163.MCT-11-0998

weight, advantages that set ELPs apart from synthetic polymers with similar properties.

Recently, Mackay and colleagues reported that conjugates of hydrophilic ELP (T_t » 42°C) and doxorubicin have enhanced antitumor activity over doxorubicin against C26 murine colon carcinoma tumors in BALB/c mice (12). However, because the ELP variant used in this study was not responsive to mild hyperthermia, the thermal targeting properties of ELP could not be exploited. Because ELP is a thermally responsive molecule, drug delivery by ELP should be enhanced in response to the temperature difference between the systemic environment and the tumor region that is exposed to hyperthermia. Therefore, we used a thermally responsive ELP1 variant (59 kDa) that has T_t close to 40°C to evaluate the enhancement of doxorubicin delivery by the application of focused mild hyperthermia on the tumor. In addition, we modified the N-terminus of ELP1 with the cell-penetrating peptide, SynB1 for enhanced intratumoral and intracellular uptake (13–15). The cell-penetrating thermally responsive SynB1-ELP1 polypeptide was conjugated to a thiol-reactive doxorubicin prodrug. This prodrug of doxorubicin, (6-maleimidocaproyl) hydrazone of doxorubicin (DOXO-EMCH, 1) binds rapidly and selectively to cysteine-34 of circulating albumin *in situ* and has marked antitumor activity in preclinical studies (16–19) and in a phase I clinical trial (20). DOXO-EMCH, meanwhile renamed INNO-206, is scheduled to enter a sarcoma phase 2 study (see www.cytrx.com).

DOXO-EMCH is a valid candidate to evaluate thermal targeting by ELP because the maleimide moiety on DOXO-EMCH allows for selective conjugation to cysteine residues at the C-terminus of ELP. In addition, the acid-sensitive hydrazone linker acts as a predetermined breaking point for ensuring effective cleavage of the drug either in the slightly acidic tumor microenvironment or after intracellular uptake in the acidic compartments of the endosomes and/or lysosomes (20). Because Doxo-EMCH delivered by SynB1-ELP ultimately results in the delivery of doxorubicin, the ELP–doxorubicin delivery system is simply referred to as SynB1-ELP-Dox. In this article, we show that thermal targeting of doxorubicin delivered by SynB1-ELP enhances its tumor uptake, plasma kinetics, and maximum-tolerated dose (MTD) compared with free doxorubicin, resulting in a potent anticancer agent capable of stabilizing disease progression.

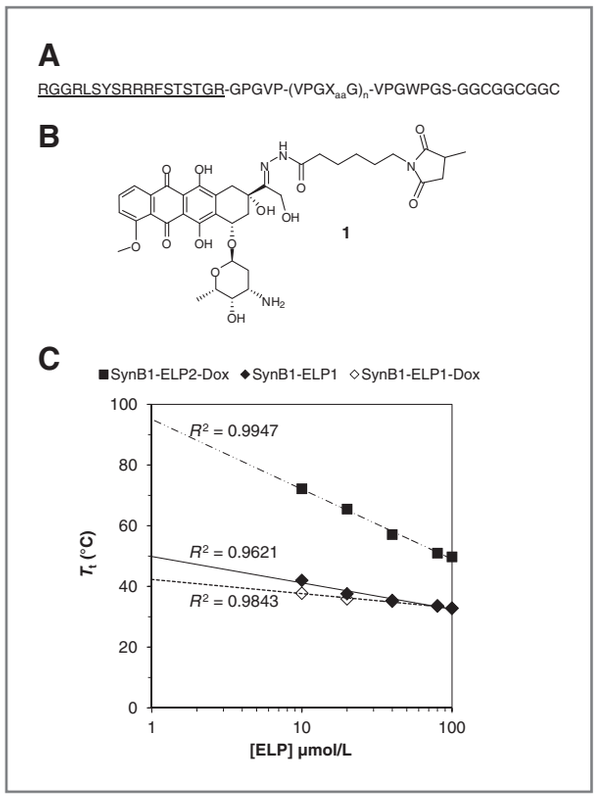

Figure 1. Characteristics of SynB1-ELP1-Dox. A, the macromolecular carrier of doxorubicin is composed of the SynB1 cell penetrating peptide (underlined), the thermally responsive biopolymer ELP, ELP1 (within parentheses, in which X_{aa} indicates a V:G:A ratio of 5:3:2 and *n* indicates 150 repeats), and 3 terminal cysteine residues where up to 3 molecules of (6-maleimidocaproyl)hydrazone derivatives of doxorubicin, 1 (B), can bind. For the thermally insensitive ELP variant, ELP2 the V:G:A ratio is 1:7:8 and *n* is 160. C, the effect of doxorubicin labeling on T_t of ELP shows a logarithmic relationship with the ELP concentration. Dox, doxorubicin.

Materials and Methods

Synthesis and conjugation of DOXO-EMCH to SynB1-ELP

The thermally responsive SynB1-ELP1 and the thermally insensitive SynB1-ELP2 constructs were cloned as described (21) with 3 Gly-Gly-Cys repeats at the C-terminus for conjugation with DOXO-EMCH (Fig. 1A). ELP2 (61 kDa, $T_t \sim 70$°C) is a size-matched control for ELP1 and is used to parse the nonspecific effects of hyperthermia (21). The polypeptides were expressed in *E. coli* using the hyperexpression protocol and purified by inverse thermal cycling (11).

Doxorubicin was derivatized at its C-13 keto position with a maleimidocaproyl hydrazide linker yielding (6-maleimidocaproyl)hydrazone derivative of doxorubicin (DOXO-EMCH, **1**, Fig. 1B) that was covalently linked to the 3 cysteine residues on ELP as described (17, 22). Briefly, the SynB1-ELP1 or SynB1-ELP2 polypeptide was conjugated to DOXO-EMCH in a Michael addition by incubating 125 μmol/L protein with 10-fold molar excess of tris-(2-carboxyethyl)phosphine (Invitrogen) at +4°C for 20 minutes and then with 4-fold molar excess of Doxo-EMCH at 27°C for 1 hour in the dark in a final volume of 10 mL of 0.1 mol/L Na_2CO_3 buffer pH 9. The majority of unreacted label was removed by inverse thermal cycling, and the drug–protein conjugate was resupsended in PBS and passed through a desalting spin column (Thermo Scientific). Doxorubicin concentration was determined using doxorubicin absorbance at 495 nm and extinction coefficient, 9,250 L/mol cm. Doxorubicin absorbance at 280 nm was factored out and the protein concentration was calculated using absorbance at 280 nm and the

protein's molar extinction coefficient, 7,190 L/mol cm based on the following equation:

$$[\text{Protein}] = \frac{(\text{Abs}_{280\text{ nm}} - (0.713 \times \text{Abs}_{495\text{ nm}}))}{7,190\text{ L/mol cm} \cdot 1\text{ cm}}$$

Thermal characterization of ELP-Dox

SynB1-ELP1 labeled with DOXO-EMCH was diluted to various concentrations of ELP in 100% serum. The solution was heated at a rate of 1°C/min from 20 to 80°C, and the resulting turbidity was measured as a function of temperature (Cary, Varian Instruments). The percentage of maximum absorbance at 600 nm was calculated for each dataset, and T_t was defined as the temperature at which 50% of the maximum was observed. T_t versus concentration curves were fitted to a logarithmic fit to estimate the thermal targeting range of the SynB1-ELP-Dox conjugates.

Cell line and tumor model

The E0771 cells originally isolated from a spontaneous cancer in C57BL/6 were obtained from Dr. F.M. Sirotnak, Memorial Sloan-Kettering Cancer Center, New York, NY (23). They are characterized as estrogen receptor–positive medullary breast adenocarcinoma and closely resemble the human disease (24). No further authentication was done for this cell line. Cells were cultured in RPMI 1640 medium (Mediatech) supplemented with 10% FBS, 100 units/mL penicillin, 100 μg/mL streptomycin, 25 μg/mL amphotericin B (Invitrogen), and 2 g/L of $NaHCO_3$ at 37°C in a humidified atmosphere containing 5% CO_2.

Female C57BL/6 mice were purchased from the National Cancer Institute. All animal experiments were conducted in accordance with the NIH Guide for the Care and Use of Laboratory Animals as approved by the University of Mississippi Medical Center Institutional Animal Care and Use Committee.

Intracellular distribution

E0771 cells at approximately 50% confluency were exposed to 40 μmol/L free doxorubicin or SynB1-ELP1-Dox for 1 minute or 20 μmol/L free doxorubicin or SynB1-ELP1-Dox for 30 or 240 minutes at 37°C. To determine the effect of temperature on doxorubicin distribution, cells were exposed to 20 μmol/L SynB1-ELP1-Dox or free doxorubicin for 1 hour at 37 or 42°C, after which the drugs were replaced with fresh medium and cells were incubated at 37°C for 24 hours. All treated cells were rinsed with PBS and fixed with 4% paraformaldehyde for 10 minutes at room temperature. After rinsing with PBS for 3 times, cells were visualized for doxorubicin fluorescence using a laser scanning confocal microscope (TS2 Leica). All treatment concentrations were based on doxorubicin equivalent.

Tumor implantation

E0771 cells grown to approximately 80% confluence were harvested by trypsin digestion. Cells were washed in PBS, counted using a Coulter counter, and diluted in PBS. With the mice under isofluorane anesthesia, 1×10^6 cells/200 μL/mouse were injected subcutaneously near the fat pad of the fourth mammary gland in the lower right abdomen.

Pharmacokinetics study

Mice bearing approximately 250 mm^3 tumors were anesthetized by isoflurane, and a Micro-Renathane catheter (Braintree Scientific) was placed in the femoral artery. Animals were intravenously injected via the femoral vein with 5 mg doxorubicin equivalent/kg of either SynB1-ELP1-Dox or free doxorubicin. Blood samples were collected over a 4-hour period via the arterial catheter in heparinized microhematocrit glass tubes. A 6-hour sample was taken at the time of euthanasia by cardiac puncture. Tumors of the animals in the hyperthermia group were heated immediately following drug administration with infrared light generated by a laser emitting diode device (Mettler Electronics) that raises the core tumor temperature to 42°C (6). The heating protocol consisted of a thermal cycling procedure with 20 minutes of heat application followed by 10 minutes of heat withdrawal repeated 4 times up to 2 hours to ensure maximum accumulation of ELP in the tumor (6, 25). Plasma from the cells was separated by centrifuging the samples at 15.7 $\times$ *g* for 5 minutes. Protein-bound doxorubicin was cleaved and extracted from plasma as described (12). Briefly, 10 μL of plasma sample was incubated with 490 μL of acidified 90% isopropanol (75 mmol/L HCl) overnight at 4°C in the dark. The isoproponal extract was collected by centrifugation at 15.7 $\times$ *g* for 10 minutes at 4°C and loaded in black 96-well plates in duplicate at 200 μL/well. Doxorubicin fluorescence was measured at 485 nm excitation and 590 nm emission in a plate reader (BioTek). The raw data were fitted to a free doxorubicin standard curve to estimate doxorubicin plasma concentration with respect to time. Plasma clearance data were fitted to a 2-compartmental model using Microcal Origin as described (6).

Biodistribution study

Doxorubicin distribution was measured using tumors and hearts harvested 6 hours after drug administration described above. Tumors and hearts were excised, snap-frozen in liquid nitrogen, and stored at −80°C. Doxorubicin concentration was determined as described (12). Briefly, tissues were weighed, suspended in 1.5 mL of acidified isopropanol, homogenized (PowerGen 125 tissue homogenizer; Fisher Scientific), and incubated overnight at +4°C with continuous mixing. Doxorubicin was extracted in the supernatant fraction by centrifugation at 15.7 $\times$ *g* for 10 minutes at +4°C. The homogenates were resuspended in 1.0 mL of 90% isopropanol, centrifuged, and the supernatant was collected. This process was repeated twice to ensure quantitative doxorubicin extraction. The supernatant fractions were evaporated to dryness in a SpeedVac concentrator. The precipitate was pooled in 600 μL of 90% isopropanol. The resulting sample was centrifuged at 15.7 $\times$ *g* for 10 minutes at 4°C to remove

tissue debris and then loaded in duplicate in black 96-well plates at 200 μL/well. Percent of injected dose per gram (%ID/g) was calculated by fitting doxorubicin fluorescence from each sample to a free doxorubicin standard curve after subtracting autofluorescence from saline control samples.

Tumor reduction at equimolar dose

Mice bearing approximately 150 mm^3 tumor were injected with 5 mg/kg doxorubicin equivalent of free doxorubicin, thermally responsive SynB1-ELP1-Dox, or thermally insensitive SynB1-ELP2-Dox on d0, d2, and d4 intravenously via the femoral vein. In addition, 280 mg/kg of SynB1-ELP1, the equivalent dose of protein present in the SynB1-ELP1-Dox treatment, was administered to the animals to rule out the toxicity of the unlabeled carrier. Animals in the hyperthermia group were heated using the heating protocol as described above. Tumor measurement ($width^2 \times length/2$) and body weight were recorded every day after treatment. Animals were sacrificed on d14, when the control tumor size reached 2,000 mm^3. Tumors were harvested and weighed after euthanasia.

Maximum-tolerated dose study

In a dose finding study, nontumor bearing mice were injected with free drug at 8, 10, 20, or 40 mg/kg, or with SynB1-ELP1-Dox at 10, 15, 20, or 40 mg/kg doxorubicin equivalent every other day 3 times via the femoral vein. In addition, to determine the effect of hyperthermia on treatment tolerance, animals bearing tumors were treated with 12 or 15 mg/kg of SynB1-ELP1-Dox (doxorubicin equivalent), followed by heating of the tumors. Animals were weighed every day to monitor the change in body weight following treatment. Mice that lost excess of 20% of their pretreatment body weight were euthanized. Animals that showed less than 20% weight loss were monitored up to a 30-day period. The highest dose at which no animal mortality and no weight loss more than 20% was observed was defined as the MTD.

Antitumor efficacy at the maximum-tolerated dose

Mice bearing tumors at approximately 150 mm^3 were injected with the MTD of free drug (8 mg/kg), or the MTD of SynB1-ELP1-Dox (12 mg/kg) on d0, d2, and d4 intravenously via the femoral vein. In addition, 650 mg/kg of SynB1-ELP1, the equivalent dose of protein present in the SynB1-ELP1-Dox treatment, was administered to the animals. Animals in the hyperthermia group were heated using the heating protocol described above. Tumor volume and body weight were measured daily up to day 14, at which point animals were sacrificed and tumors were harvested and weighed.

Statistical analysis

A one-way ANOVA with Bonferroni tests for pair-wise comparison of treatment groups was done to analyze the statistical differences between the treatment groups and the untreated control.

Results and Discussion

Thermal characterization of SynB1-ELP-Dox

To attach the cargo drug DOXO-EMCH to ELP, we designed 3 cysteine residues at the carboxy terminus of ELP that were separated by diglycine spacers (Fig. 1A). The cysteines ideally allowed for conjugation of up to 3 molecules of DOXO-EMCH, whereas the diglycine spacers ensured that Doxo-EMCH attachment was carried out with minimum steric hindrance. A Michael addition of DOXO-EMCH to ELP resulted in an average molar label ratio of 2.10. A turbidity assay done to determine the effect of drug labeling on ELP phase transition showed a logarithmic relationship between T_t and concentration of ELP. Although the attachment of Doxo-EMCH to SynB1-ELP1 decreased the T_t slightly, SynB1-ELP-Dox T_t remained above 37°C in the lower micromolar range suitable for thermal targeting in animals (Fig. 1C). At the same time, the T_t of SynB1-ELP2-Dox was detected at $T \gg 37$°C, confirming that it is a suitable control to assess the nonspecific effect of hyperthermia.

SynB1-ELP1-Dox intracellular distribution

Previous studies with conjugates of DOXO-EMCH and albumin have shown that doxorubicin does not enter the nucleus but localizes in the cytoplasm, primarily in mitochondria and Golgi apparatus (26). Therefore, we evaluated the subcellular distribution of Doxo-EMCH delivered by SynB1-ELP1 by confocal microscopy. Doxorubicin delivered by SynB1-ELP1 exhibited a time-dependent nuclear distribution compared with free doxorubicin that displayed nuclear localization immediately after treatment (Fig. 2A–B). In this time course experiment, 1 minute after exposure, doxorubicin delivered by SynB1-ELP1 was mainly detected in the cytoplasm or on the outer surface of the cell, whereas free doxorubicin localized primarily in the nucleus. Although some doxorubicin from SynB1-ELP1 was still detected in the cytoplasm after 30 minutes of exposure, by 4 hours almost all of doxorubicin from SynB1-ELP1 was found in the nucleus. Interestingly, the distribution of free doxorubicin shifted from an exclusively nuclear localization after 30 minutes to both nuclear and cytoplasmic distribution by 4 hours, which is similar to other findings (26). Furthermore, addition of hyperthermia did not alter the nuclear distribution of doxorubicin delivered by SynB1-ELP1, as doxorubicin fluorescence was detected in the nucleus even after 24 hours posttreatment (Fig. 2C). The SynB1 peptide is derived from the protegrin family of antimicrobial peptides and is known to facilitate cellular uptake of its cargo by adsorptive-mediated endocytosis (27), which likely places the ELP-Dox conjugates inside the acidic environment of endosomes/lysosomes where the cleavage of the acid-labile hydrazone linker releases doxorubicin inside the cell.

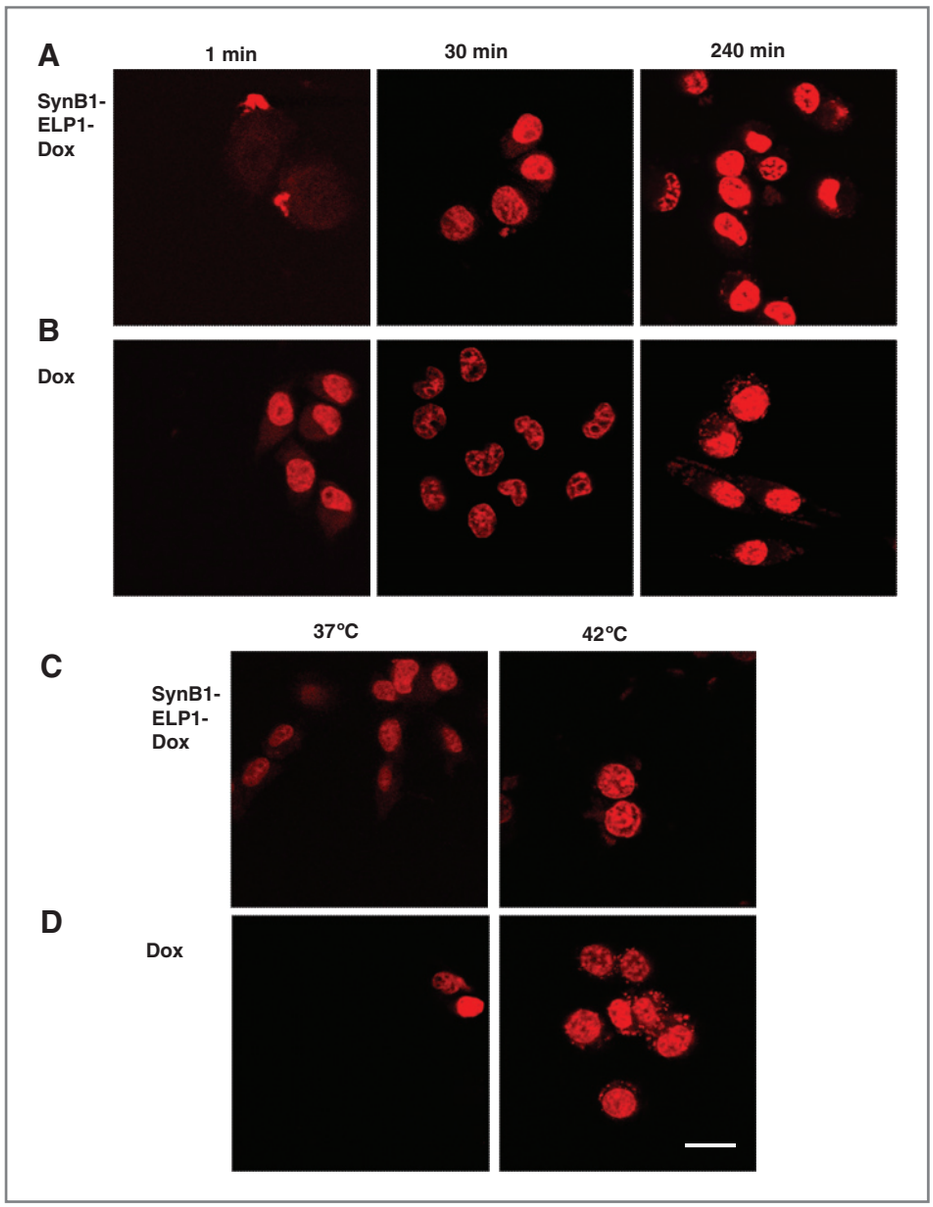

Figure 2. Delivery of doxorubicin to the nucleus by SynB1-ELP1. Laser scanning confocal images of E0771 cells exposed to SynB1-ELP1-Dox (A) or free doxorubicin (B) at 40 μmol/L doxorubicin equivalent for 1 minute or 20 μmol/L doxorubicin equivalent for 30 minutes and 4 hours show a time-dependent nuclear distribution of doxorubicin delivered by SynB1-ELP1. In addition, images of E0771 cells exposed to SynB1-ELP1-Dox (C) or free doxorubicin (D) at 20 μmol/L doxorubicin equivalent for 1 hour at 37°C or 42°C indicate that hyperthermia does not affect the distribution of doxorubicin delivered by SynB1-ELP1. Scale bar, 20 μm. Dox, doxorubicin.

The cytoplasmic distribution of SynB1-ELP1 observed in a previous study (15) and the results of this data indicate that doxorubicin is being cleaved from the ELP carrier intracellularly and being diffused to the nucleus where it acts in analogy to free doxorubicin.

SynB1-ELP1-Dox pharmacokinetics and tumor distribution

Because unmodified ELP1 has a terminal plasma half-life of nearly 8 hours (9), we evaluated the pharmacokinetics of SynB1-ELP1-Dox to determine whether it could also extend the plasma half-life of doxorubicin. As anticipated, SynB1-ELP1-Dox displayed a biphasic doxorubicin clearance and a longer systemic circulation presence (Fig. 3A). In contrast, free drug displayed a rapid plasma clearance with relatively lower plasma concentrations (Fig. 3B). Because we were only able to observe the distribution phase of free doxorubicin using our assay method, the terminal half-life of SynB1-ELP1-Dox was compared with that of free doxorubicin values from the literature. Whereas the fit of SynB1-ELP1-Dox with no hyperthermia yielded a terminal half-life of 305.5 ± 40.5 minutes, the fit of SynB1-ELP1-Dox in combination with hyperthermia yielded a terminal half-life of 336.5 ± 70.2 minutes (Supplementary Table S1). The reported terminal half-life of doxorubicin in C57BL/6 mice is 31.8 minutes (28), nearly 10-fold faster than ELP-conjugated doxorubicin, suggesting that ELP conjugation with doxorubicin extends its systemic circulation time compared with free doxorubicin.

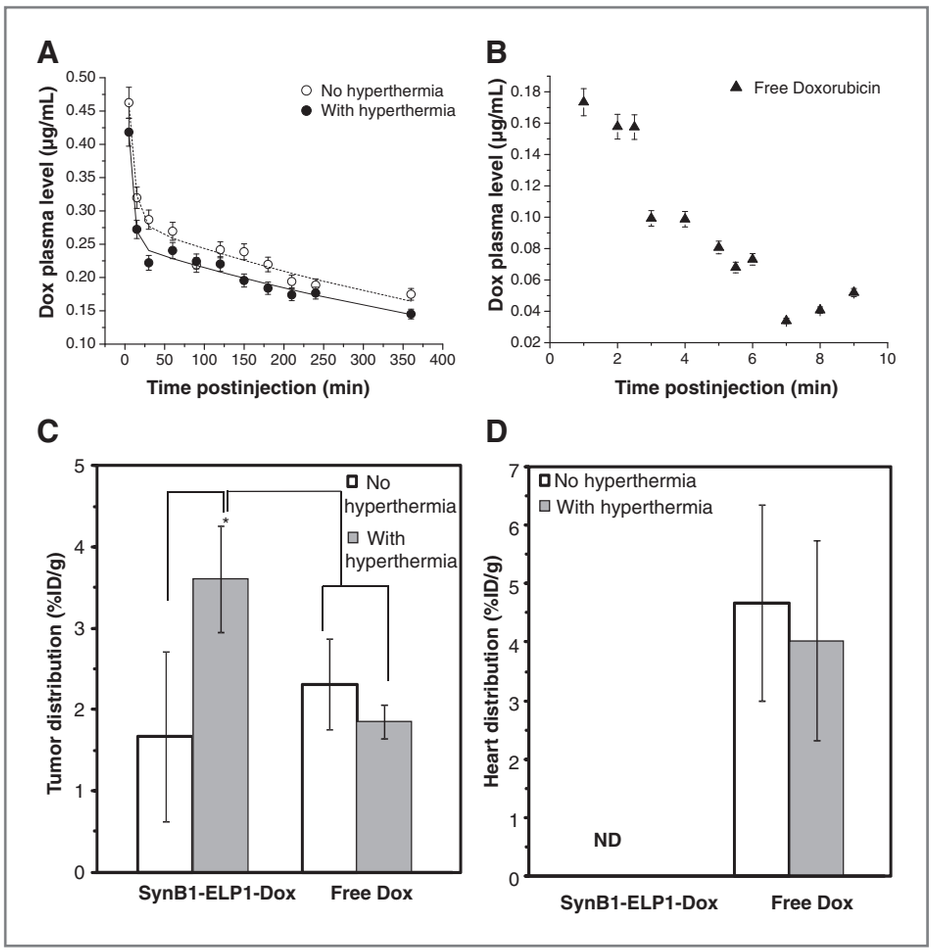

Figure 3. Pharmacokinetics and tissue distribution of SynB1-ELP1-Dox. C57BL/6 black mice were treated with either 5 mg doxorubicin equivalent/kg of either SynB1-ELP1-Dox in the absence or presence of hyperthermia or free doxorubicin. A, doxorubicin plasma concentration after SynB1-ELP1-Dox treatment was fitted to a 2-compartment model. B, due to relatively faster plasma clearance and lower detectable plasma concentrations, the plasma clearance of free doxorubicin could only be confirmed up to 10 minutes; therefore, the pharmacokinetics data of free doxorubicin (28) was used for comparison with SynB1-ELP1-Dox. Doxorubicin concentration in tumors (C) and hearts (D) at 6 hours postinjection. *, $P < 0.01$ (ANOVA, Bonferroni contrast, mean $\pm$ SD; $n = 5$). ND indicates that doxorubicin fluorescence signal was not detected over the control background. Dox, doxorubicin.

To evaluate whether doxorubicin tumor levels were enhanced by thermal targeting of ELP over free doxorubicin, tumor samples were analyzed for doxorubicin fluorescence. In addition, because doxorubicin accumulation in the heart is a major concern, we also assayed heart samples from the treated animals. With respect to doxorubicin levels in the tumor, more than 2-fold increase in doxorubicin uptake was observed after SynB1-ELP1-Dox treatment in combination with hyperthermia compared with treatment with only free drug (Fig. 3C). Thermal targeting with SynB1-ELP1 also significantly enhanced doxorubicin uptake in the tumor by a factor of 2 compared with when no hyperthermia was applied (Fig. 3C), indicating that hyperthermia is necessary for increased tumor accumulation of SynB1-ELP1-Dox. This is because application of hyperthermia at the tumor site causes ELP1 to phase transition into aggregates, which essentially pools it in the tumor microenvironment. The thermal cycling hyperthermia application protocol, in which the heat source is applied and withdrawn periodically, ensures that the aggregates trapped in the tumor vasculature resolubilize and diffuse into the tumor extravascular space (25). Subsequently, the SynB1 moiety on ELP1 facilitates its endocytosis in the tumor cells (13). Therefore, the function of hyperthermia is to maximize the local concentration of ELP that is delivered inside the tumor cells (6, 14, 15).

With respect to doxorubicin levels in the heart, the fluorescence intensity of doxorubicin from animals treated with SynB1-ELP1-Dox could not be detected over the control background signal. However, at the same dose of free doxorubicin, we detected high levels of doxorubicin in the heart (Fig. 3D). Given that doxorubicin-related cardiotoxcitiy is a dose-limiting side effect, this observation can have meaningful implications in the therapeutic use of ELP-Dox. We expect that through the means of thermal targeting, ELP-Dox can potentially reduce cardiotoxicity of doxorubicin by steering it away from the heart and targeting it to the tumor. This is further supported by the findings that chronic treatment with DOXO-EMCH resulted in reduced cardiomyopathy compared with free doxorubicin in rats (19).

Hyperthermia enhances tumor inhibition by SynB1-ELP1-Dox

The antitumor potential of SynB1-ELP1-Dox in combination with hyperthermia was evaluated and compared with that of standard doxorubicin at an equimolar dose of

Table 1. Maximum-tolerated dose

Treatment (d0, d2, d4)	Dose[a] (mg/kg)	Day of >20% of pretreatment body weight loss[b]	Number of survivors/ Sample size
SynB1-ELP1-Dox no hyperthermia	10	–	3/3
	15	–	3/3
	20	5, 5, 5	0/3
	40	3, 3, 3	0/3
SynB1-ELP1-Dox with hyperthermia	12	–	5/5
	15	3, 4, 5	0/3
Free Dox	8	–	3/3
	10	0, 2	4/6
	20	0, 2, 4	0/3
	40	2, 3, 3	0/3
	Vehicle[c]	–	3/3

[a]Doxorubicin equivalent.
[b]Individual animal.
[c]Eight percent dimethyl sulfoxide–phosphate buffer.

5 mg/kg given on days 0, 2, and 4. Fourteen days after treatment, mice treated with SynB1-ELP1-Dox in conjunction with hyperthermia had a mean tumor volume that was nearly 4-fold smaller than the saline-treated control tumors and nearly 2.5-fold smaller than the SynB1-ELP1-Dox without hyperthermia-treated group (Fig. 4A). In the presence of hyperthermia, both SyB1-ELP1-Dox and free doxorubicin exerted similar antitumor effect. A 2-fold

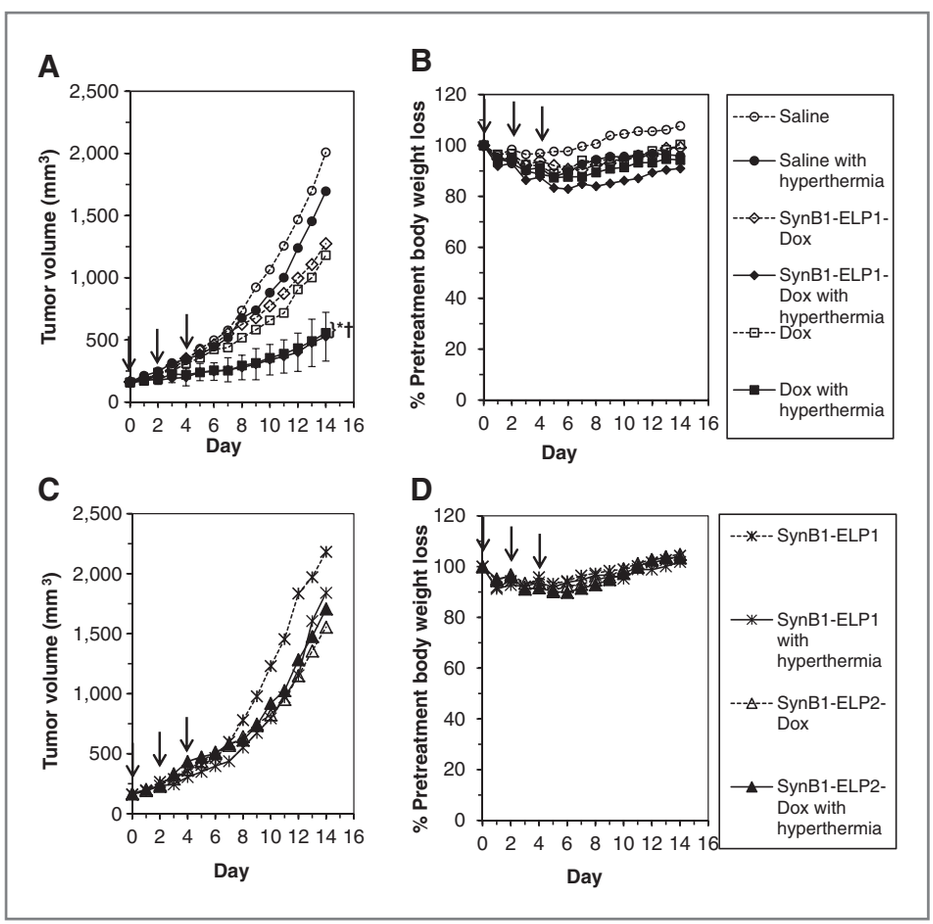

Figure 4. Hyperthermia enhances the antitumor activity of SynB1-ELP1-Dox. Tumor-bearing mice were intravenously injected with saline (A, B), 5 mg/kg of doxorubicin equivalent of SynB1-ELP1-Dox or free doxorubicin, or SynB1-ELP2-Dox or SynB1-ELP1 (C, D) on d0, d2, and d4 (↓); mean ± SD, $n = 6$–10. Tumor volume (A, C) and body weight (B, D) in response to treatment up to day 14 are shown. * indicates significant difference between treatment and saline control at 37°C, $P < 0.0001$. Dox, doxorubicin.

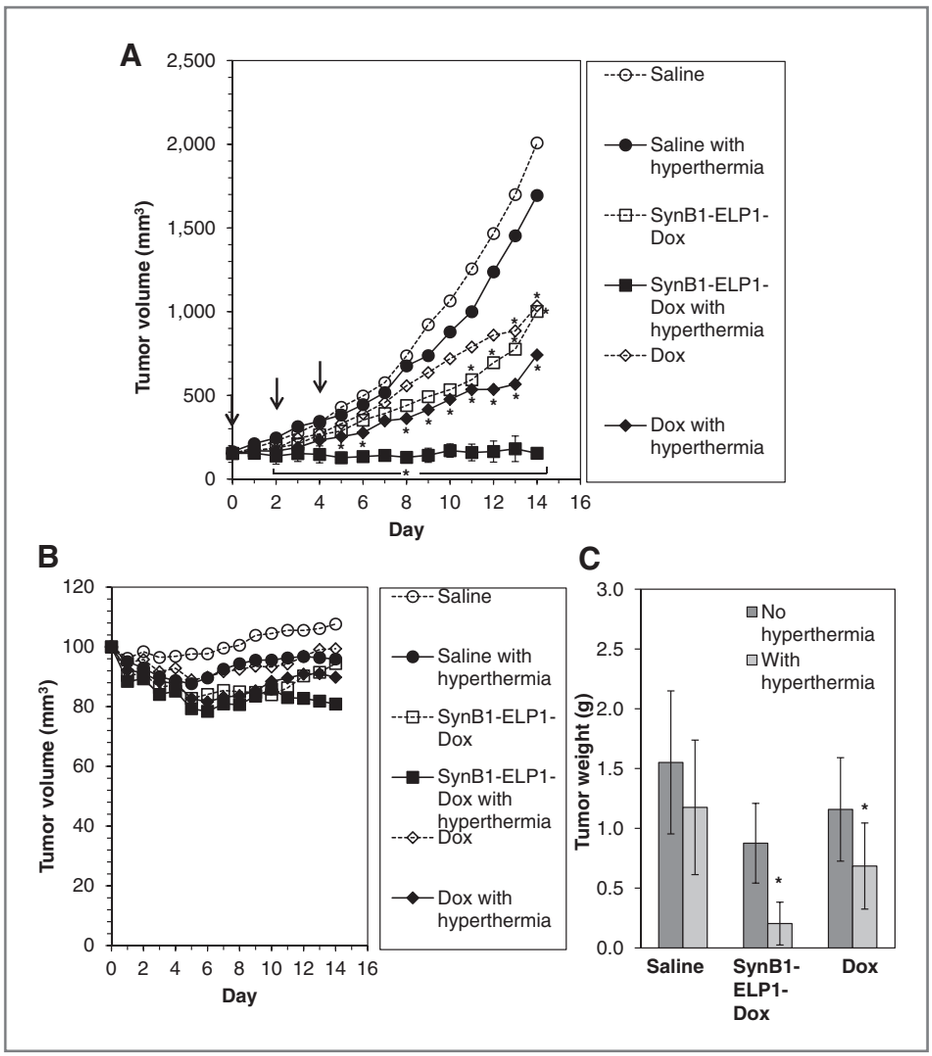

Figure 5. At the MTD, SynB1-ELP1-Dox in combination with hyperthermia completely inhibits tumor growth. Tumor-bearing animals were treated on d0, d2, and d4 (↓) at the MTD with saline with or without hyperthermia, free doxorubicin (8 mg/kg) with or without hyperthermia, and SynB1-ELP1-Dox (12 mg/kg) with or without hyperthermia; mean ± SD, $n = 6$–10. Tumor size (A) and body weight (B) was measured daily up to 14 days after treatment. C, animals were sacrificed 14 days after treatment, and the tumors were harvested and weighed. * indicates significant difference between treatment and saline control at 37°C, $P < 0.001$. Dox, doxorubicin.

enhancement of antitumor activity of free doxorubicin was seen in the presence of hyperthermia compared with when no hyperthermia was used. This could be explained by the synergistic effect of hyperthermia on doxorubicin toxicity through increased perfusion and vascular fenestration (29–31). However, at the same dose, the thermally insensitive variant SynB1-ELP2-Dox had no effect on tumor inhibition either in the presence or absence of hyperthermia (Fig. 4C), indicating that hyperthermia-mediated aggregation of ELP1 is necessary for the enhanced antitumor activity of SynB1-ELP1-Dox. This also underlies possibly difference in response of free doxorubicin versus doxorubicin conjugated to SynB1-ELP to hyperthermia. Furthermore, the protein carrier SynB1-ELP1 had no effect on tumor inhibition compared with the untreated control (Fig. 4C), indicating that the carrier is nontoxic. Most importantly, under our heating protocol, hyperthermia alone had no effect on tumor growth. Tumor weights from these animals correlated with the tumor growth curve data (Supplementary Fig. 1S). Body weight change in response to treatment was observed well above the 80% pretreatment weight limit, indicating that the animals are able to tolerate the therapy (Fig 4B and D).

Maximum-tolerated dose of SynB1-ELP1-Dox

Even though SynB1-ELP1–delivered doxorubicin and free doxorubicin had similar potencies for tumor reduction in equimolar comparison (Fig. 4), we expected that the ELP-fused form of the drug would have higher a MTD. On the basis of our definition of MTD, both free doxorubicin and SynB1-ELP1-Dox were found to be highly toxic at a dose higher than 20 mg/kg doxorubicin equivalent (Table 1). Treatment with 10 mg/kg free doxorubicin did not result in complete survival. However, at 8 mg/kg all the free doxorubicin-treated animals survived with weight loss less than 20%. Thus, the MTD of free doxorubicin was set at 8 mg/kg. Animals were able to tolerate both 10 and 15 mg/kg of SynB1-ELP1-Dox treatments (Table 1). To evaluate the effect of hyperthermia on the MTD of SynB1-ELP1-Dox, tumor-bearing animals were

used so that focused heat could be applied to the tumor. In conjunction with hyperthermia, a dose of 15 mg/kg of SynB1-ELP1-Dox was poorly tolerated by the animals. At a slightly lower dose of 12 mg/kg, however, animal tolerance of the treatment was acceptable, resulting in a complete survival (Table 1). Therefore, the MTD of SynB1-ELP1-Dox was set at 12 mg/kg. However, this dose was given 3 times so that the cumulative dose of SynB1-ELP1-Dox was 36 mg/kg (Table 1). Although the ELP-Dox designed by Mackay and colleagues had an MTD of 20 mg/kg (12), this dose was only given once indicating that SynB1-ELP1-Dox is better tolerated, which may be due to the enhanced ELP tumor penetration mediated by SynB1.

Complete tumor inhibition by SynB1-ELP1-Dox

The therapeutic efficacy of SynB1-ELP1-Dox against the E0771 murine breast tumors was evaluated and compared with free doxorubicin at the respective MTD. Fourteen days after the start of the treatment, the mean tumor volume of the animals treated with SynB1-ELP1-Dox without hyperthermia was at 1,002 mm^3 and 6.5-fold smaller at 154 mm^3 when combined with hyperthermia. This was also significantly smaller than the saline-treated control tumors by nearly 13-fold (Fig. 5A). Under hyperthermic condition, SynB1-ELP1-Dox outperformed free doxorubicin by approximately 5-fold, resulting in a complete inhibition of tumor progression (Fig. 5A). In contrast, free doxorubicin resulted in partial tumor inhibition. Overt toxicity was not evident in the treated animals (Fig. 5B). Tumor weight data from the treated animals were consistent with the tumor growth curve (Fig. 5C). Furthermore, the drug-free carrier SynB1-ELP1 did not have any effect on tumor inhibition (data not shown) either with or without hyperthermia, indicating that the ELP vector by itself is nontoxic. The cumulative effect of improved pharmacokinetics, enhanced tumor uptake, and concomitant increase of MTD of SynB1-ELP1-Dox over free doxorubicin resulted in a significant enhancement in the efficacy of SynB1-ELP1-Dox compared with the free drug.

In conclusion, thermal targeting of SynB1-ELP1-Dox resulted in complete tumor growth inhibition and substantially higher therapeutic benefit of the drug in an animal model that is otherwise partially responsive to standard doxorubicin treatment. To the best of our knowledge, this is the first preclinical demonstration of thermal targeting of a chemotherapeutic using the ELP carrier system. The advantage of combining hyperthermia with ELP is that hyperthermia increases permeability of tumor vasculature compared with normal vasculature, resulting in enhanced extravasation of macromolecules (32–34) and enhanced cellular uptake (35, 36). Furthermore, due to the built-in acid-labile linker on Doxo-EMCH, delivery by SynB1-ELP ensures that the drug is released inside the cells. In contrast, liposomal formulation of doxorubicin such as poly(ethylene glycol)-encapsulated liposomal doxorubicin (PEG-Dox; Doxil), although has superior therapeutic efficacy compared with standard doxorubicin (37), shows mostly perivascular accumulation and limited tumor uptake (38). In addition, cellular delivery of the drug depends on the release of the drug from the liposomes, which in turn depends on the concentration gradient between the tumor vasculature and the extravascular space. Our current findings encourage us to evaluate the ELP drug delivery system in other tumor-bearing models to optimize the hyperthermia regimen to obtain tumor regressions. Tumor-specific SynB1-ELP-Dox could have an important impact in tumors that respond poorly to standard doxorubicin, and the potential to be combined in multimodal cancer therapy. Furthermore, because the use of hyperthermia is already established in clinical practice, precise heating of deep-seated tissues can extend thermal targeting of ELPs to internal organs as well (reviewed in refs. 39–41).

Disclosure of Potential Conflicts of Interest

D. Raucher is the president of and has ownership interest (including patents) in Thermally Targeted Therapeutics, Inc.

Authors' Contributions

Conception and design: S. Moktan, D. Raucher
Development of methodology: S. Moktan, E. Perkins, D. Raucher
Acquisition of data (provided animals, acquired and managed patients, provided facilities, etc.): S. Moktan, E. Perkins, D. Raucher
Analysis and interpretation of data (e.g., statistical analysis, biostatistics, computational analysis): S. Moktan, D. Raucher
Writing, review, and/or revision of the manuscript: S. Moktan, E. Perkins, F. Kratz, D. Raucher
Administrative, technical, or material support (i.e., reporting or organizing data, constructing databases): F. Kratz
Study supervision: E. Perkins, D. Raucher

Acknowledgments

The authors thank Dr. Susan Wellman for help with the pharmacokinetics analysis, Dr. Gene L. Bidwell III for critical reading of the manuscript, and Ms. Maria Brady, Ms. Rowshan Begum, and Ms. Rebecca Singleterry for technical assistance.

Grant Support

This work was supported by grants from the National Science Foundation (CBET-931041) and NIH (1R21CA137418-01A2 and 1R21CA139589-01) to D. Raucher.

The costs of publication of this article were defrayed in part by the payment of page charges. This article must therefore be hereby marked *advertisement* in accordance with 18 U.S.C. Section 1734 solely to indicate this fact.

Received December 7, 2011; revised March 23, 2012; accepted April 16, 2012; published OnlineFirst April 24, 2012.

References

1. Raucher D, Massodi I, Bidwell GL. Thermally targeted delivery of chemotherapeutics and anti-cancer peptides by elastin-like polypeptide. Expert Opin Drug Deliv 2008;5:353–69.
2. Bidwell GL 3rd, Davis AN, Fokt I, Priebe W, Raucher D. A thermally targeted elastin-like polypeptide-doxorubicin conjugate overcomes drug resistance. Invest New Drugs 2007;25:313–26.

3. Bidwell GL 3rd, Fokt I, Priebe W, Raucher D. Development of elastin-like polypeptide for thermally targeted delivery of doxorubicin. Biochem Pharmacol 2007;73:620–31.
4. Dreher MR, Raucher D, Balu N, Michael Colvin O, Ludeman SM, Chilkoti A. Evaluation of an elastin-like polypeptide-doxorubicin conjugate for cancer therapy. J Control Release 2003;91:31–43.
5. Chilkoti A, Dreher MR, Meyer DE, Raucher D. Targeted drug delivery by thermally responsive polymers. Adv Drug Deliv Rev 2002;54:613–30.
6. Bidwell GL 3rd, Perkins E, Raucher D. A thermally targeted c-Myc inhibitory polypeptide inhibits breast tumor growth. Cancer Lett 2012;319:136–43.
7. Yamaoka T, Tamura T, Seto Y, Tada T, Kunugi S, Tirrell DA. Mechanism for the phase transition of a genetically engineered elastin model peptide (VPGIG)40 in aqueous solution. Biomacromolecules 2003;4:1680–5.
8. Meyer DE, Chilkoti A. Quantification of the effects of chain length and concentration on the thermal behavior of elastin-like polypeptides. Biomacromolecules 2004;5:846–51.
9. Liu W, Dreher MR, Furgeson DY, Peixoto KV, Yuan H, Zalutsky MR, et al. Tumor accumulation, degradation and pharmacokinetics of elastin-like polypeptides in nude mice. J Control Release 2006;116:170–8.
10. Maeda H, Seymour LW, Miyamoto Y. Conjugates of anticancer agents and polymers: advantages of macromolecular therapeutics *in vivo*. Bioconjug Chem 1992;3:351–62.
11. Bidwell GL 3rd, Raucher D. Application of thermally responsive polypeptides directed against c-Myc transcriptional function for cancer therapy. Mol Cancer Ther 2005;4:1076–85.
12. MacKay JA, Chen M, McDaniel JR, Liu W, Simnick AJ, Chilkoti A. Self-assembling chimeric polypeptide-doxorubicin conjugate nanoparticles that abolish tumours after a single injection. Nat Mater 2009;8:993–9.
13. Rousselle C, Clair P, Lefauconnier JM, Kaczorek M, Scherrmann JM, Temsamani J. New advances in the transport of doxorubicin through the blood-brain barrier by a peptide vector-mediated strategy. Mol Pharmacol 2000;57:679–86.
14. Bidwell GL 3rd, Raucher D. Cell penetrating elastin-like polypeptides for therapeutic peptide delivery. Adv Drug Deliv Rev 2010;62:1486–96.
15. Bidwell GL 3rd, Whittom AA, Thomas E, Lyons D, Hebert MD, Raucher D. A thermally targeted peptide inhibitor of symmetrical dimethylation inhibits cancer-cell proliferation. Peptides 2010;31:834–41.
16. Graeser R, Esser N, Unger H, Fichtner I, Zhu A, Unger C, et al. INNO-206, the (6-maleimidocaproyl hydrazone derivative of doxorubicin), shows superior antitumor efficacy compared to doxorubicin in different tumor xenograft models and in an orthotopic pancreas carcinoma model. Invest New Drugs 2010;28:14–9.
17. Kratz F, Warnecke A, Scheuermann K, Stockmar C, Schwab J, Lazar P, et al. Probing the cysteine-34 position of endogenous serum albumin with thiol-binding doxorubicin derivatives. Improved efficacy of an acid-sensitive doxorubicin derivative with specific albumin-binding properties compared to that of the parent compound. J Med Chem 2002;45:5523–33.
18. Kratz F, Ehling G, Kauffmann HM, Unger C. Acute and repeat-dose toxicity studies of the (6-maleimidocaproyl)hydrazone derivative of doxorubicin (DOXO-EMCH), an albumin-binding prodrug of the anticancer agent doxorubicin. Hum Exp Toxicol 2007;26:19–35.
19. Lebrecht D, Geist A, Ketelsen UP, Haberstroh J, Setzer B, Kratz F, et al. The 6-maleimidocaproyl hydrazone derivative of doxorubicin (DOXO-EMCH) is superior to free doxorubicin with respect to cardiotoxicity and mitochondrial damage. Int J Cancer 2007;120:927–34.
20. Kratz F. DOXO-EMCH (INNO-206): the first albumin-binding prodrug of doxorubicin to enter clinical trials. Expert Opin Investig Drugs 2007;16:855–66.
21. Moktan S, Ryppa C, Kratz F, Raucher D. A thermally responsive biopolymer conjugated to an acid-sensitive derivative of paclitaxel stabilizes microtubules, arrests cell cycle, and induces apoptosis. Invest New Drugs 2012;30:236–48.
22. Di Stefano G, Lanza M, Kratz F, Merina L, Fiume L. A novel method for coupling doxorubicin to lactosaminated human albumin by an acid sensitive hydrazone bond: synthesis, characterization and preliminary biological properties of the conjugate. Eur J Pharm Sci 2004;23:393–7.
23. Dunham LJ, Stewart HL. A survey of transplantable and transmissible animal tumors. J Natl Cancer Inst 1953;13:1299–377.
24. Ewens A, Mihich E, Ehrke MJ. Distant metastasis from subcutaneously grown E0771 medullary breast adenocarcinoma. Anticancer Res 2005;25:3905–15.
25. Dreher MR, Liu W, Michelich CR, Dewhirst MW, Chilkoti A. Thermal cycling enhances the accumulation of a temperature-sensitive biopolymer in solid tumors. Cancer Res 2007;67:4418–24.
26. Beyer U, Rothern-Rutishauser B, Unger C, Wunderli-Allenspach H, Kratz F. Differences in the intracellular distribution of acid-sensitive doxorubicin-protein conjugates in comparison to free and liposomal formulated doxorubicin as shown by confocal microscopy. Pharm Res 2001;18:29–38.
27. Rousselle C, Smirnova M, Clair P, Lefauconnier JM, Chavanieu A, Calas B, et al. Enhanced delivery of doxorubicin into the brain via a peptide-vector-mediated strategy: saturation kinetics and specificity. J Pharmacol Exp Ther 2001;296:124–31.
28. Xiong XB, Huang Y, Lu WL, Zhang H, Zhang X, Zhang Q. Enhanced intracellular uptake of sterically stabilized liposomal Doxorubicin *in vitro* resulting in improved antitumor activity *in vivo*. Pharm Res 2005;22:933–9.
29. Yarmolenko PS, Zhao Y, Landon C, Spasojevic I, Yuan F, Needham D, et al. Comparative effects of thermosensitive doxorubicin-containing liposomes and hyperthermia in human and murine tumours. Int J Hyperthermia 2010;26:485–98.
30. Hahn GM, Braun J, Har-Kedar I. Thermochemotherapy: synergism between hyperthermia (42–43 degrees) and adriamycin (of bleomycin) in mammalian cell inactivation. Proc Natl Acad Sci U S A 1975;72:937–40.
31. Herman TS. Temperature dependence of adriamycin, cis-diamminedichloroplatinum, bleomycin, and 1,3-bis(2-chloroethyl)-1-nitrosourea cytotoxicity *in vitro*. Cancer Res 1983;43:517–20.
32. Issels RD. Regional hyperthermia combined with systemic chemotherapy of locally advanced sarcomas: preclinical aspects and clinical results. Recent Results Cancer Res 1995;138:81–90.
33. Feyerabend T, Steeves R, Wiedemann GJ, Richter E, Robins HI. Rationale and clinical status of local hyperthermia, radiation, and chemotherapy in locally advanced malignancies. Anticancer Res 1997;17:2895–7.
34. van Vulpen M, Raaymakers BW, de Leeuw AA, van de Kamer JB, van Moorselaar RJ, Hobbelink MG, et al. Prostate perfusion in patients with locally advanced prostate carcinoma treated with different hyperthermia techniques. J Urol 2002;168:1597–602.
35. Raucher D, Chilkoti A. Enhanced uptake of a thermally responsive polypeptide by tumor cells in response to its hyperthermia-mediated phase transition. Cancer Res 2001;61:7163–70.
36. Massodi I, Raucher D. A thermally responsive Tat-elastin-like polypeptide fusion protein induces membrane leakage, apoptosis, and cell death in human breast cancer cells. J Drug Target 2007;15:611–22.
37. Vail DM, Amantea MA, Colbern GT, Martin FJ, Hilger RA, Working PK. Pegylated liposomal doxorubicin: proof of principle using preclinical animal models and pharmacokinetic studies. Semin Oncol 2004;31:16–35.
38. Gabizon A, Shmeeda H, Barenholz Y. Pharmacokinetics of pegylated liposomal Doxorubicin: review of animal and human studies. Clin Pharmacokinet 2003;42:419–36.
39. Falk MH, Issels RD. Hyperthermia in oncology. Int J Hyperthermia 2001;17:1–18.
40. Dewhirst MW, Prosnitz L, Thrall D, Prescott D, Clegg S, Charles C, et al. Hyperthermic treatment of malignant diseases: current status and a view toward the future. Semin Oncol 1997;24:616–25.
41. Takahashi I, Emi Y, Hasuda S, Kakeji Y, Maehara Y, Sugimachi K. Clinical application of hyperthermia combined with anticancer drugs for the treatment of solid tumors. Surgery 2002;131:S78–84.